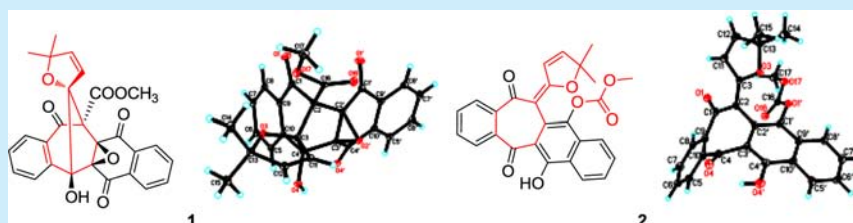


New Cytotoxic Naphthohydroquinone Dimers from *Rubia alata*Si-Meng Zhao,^{†,‡,§} Zhe Wang,^{†,‡,§} Guang-Zhi Zeng,^{*,†} Wei-Wu Song,[†] Xiao-Qiang Chen,[†] Xiao-Nian Li,[†] and Ning-Hua Tan^{*,†}[†]State Key Laboratory of Phytochemistry and Plant Resources in West China, Kunming Institute of Botany, Chinese Academy of Sciences, Kunming 650201, China[‡]University of Chinese Academy of Sciences, Beijing 100049, China

Supporting Information



ABSTRACT: Two novel naphthohydroquinone dimers with unprecedented skeletons, rubialatins A (1) and B (2), were isolated from the herbal plant *Rubia alata* together with their precursor, mollugin (3). The structures were elucidated on the basis of NMR spectra and crystal X-ray diffraction. Compound 1, a racemate, was separated by chiral column chromatography, and the absolute configurations of the enantiomers were determined by the computational methods. Cytotoxicity of 1–3 was evaluated as well as the effect on the NF- κ B pathway. Compound (+)-1 showed cytotoxicity and could inhibit NF- κ B pathway. Meanwhile, 2 showed cytotoxicity and a synergistic effect with TNF- α on NF- κ B activation.

The roots and rhizomes of *Rubia* plants (Rubiaceae) are widely used for the treatment of menoxenia, rheumatism, contusion, and tuberculosis in China, Japan, Korea, and India. Bicyclic hexapeptides,^{1–8} quinones,^{9–14} and arborinane-type triterpenoids^{9,14,15} have been isolated from *Rubia* plants. To date, six naphthohydroquinone dimers have been reported from this genus,^{11–13} and some have attracted great interest from synthetic chemists,^{16,17} for their distinctive molecular architectures.

Morphologically, *Rubia alata* Roxb. has already been distinguished from other *Rubia* plants by having linear or lanceolate leaves, while other species typically have ovate leaves. The species distributes widely in South China and has been used as a folk medicine, but no chemical investigation on this plant has been reported. In our search for bioactive secondary metabolites, two novel naphthohydroquinone dimers with unprecedented skeletons, rubialatins A (1) and B (2) and their precursor, mollugin (3) (Figure 1),¹⁰ were isolated from the roots and rhizomes of *R. alata*. Compound 1 has a novel 6/6/5/6/6 carbon skeleton coupled with a spirocycloisopentene group; 2 has a rearranged 6/7/6/6 tetracyclic system. To the best of our knowledge, no other structures with these skeletons have been reported.

Compound 1 was obtained as light yellowish crystals (acetone). Its molecular formula was determined by HREIMS ($[M]^+$, 472.1148, calcd 472.1158) as $C_{27}H_{20}O_8$, which was in accordance with the 1H and ^{13}C NMR spectroscopic data (Table 1). The IR spectrum showed the absorptions at 3525, 3442, 1732, 1712, 1599 cm^{-1} , indicating the existence of hydroxyl, carbonyl, and phenyl groups. The 1H NMR spectrum

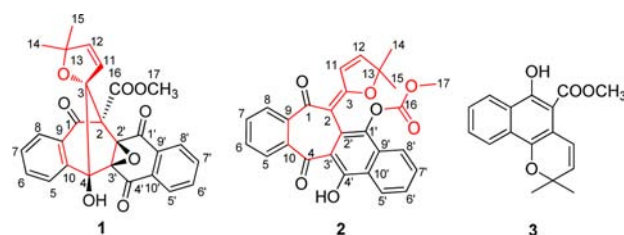


Figure 1. Structures of rubialatins A and B (1 and 2) and mollugin (3).

showed two pairs of AA'BB' type aromatic protons at δ_H 8.69 (1H, d, $J = 7.7$ Hz), 8.12 (1H, d, $J = 7.7$ Hz), 7.62 (1H, t, $J = 7.7$ Hz), 7.19 (1H, overlap), and 7.77 (2H, overlap), 7.43 (2H, overlap); two *cis* olefinic protons at δ_H 6.36 (1H, d, $J = 5.7$ Hz), 6.26 (1H, d, $J = 5.7$ Hz); one hydroxyl group at δ_H 9.63 (1H, s); one methoxyl group at δ_H 3.82 (3H, s); and two methyl groups at δ_H 1.35 (6H, 3H each, s). The ^{13}C NMR spectrum displayed three unsaturated ketonic carbonyl groups at δ_C 187.6 (s), 187.5 (s), and 186.8 (s); one carbonyl group at δ_C 166.4 (s); 12 aromatic carbons at δ_C 144.3 (s), 134.1 (d), 131.8 (s), 128.6 (d), 127.9 (d), 127.7 (d), and 134.9 (d), 134.8 (d), 133.0 (s), 132.7 (s), 127.4 (d), 127.1 (d); two olefinic carbons at δ_C 142.3 (d), 125.7 (d); one methoxyl group at δ_C 52.3 (q); two methyl groups at δ_C 28.9 (q), 27.5 (q); as well as six quaternary carbons at δ_C 102.8 (s), 88.5 (s), 81.6 (s), 69.8 (s), 68.8 (s),

Received: September 3, 2014

Published: October 13, 2014

Table 1. NMR Spectroscopic Data of Rubialatins A (1) and B (2)

position	1 ^a		2 ^b	
	δ_{H} (500 MHz)	δ_{C} (100 MHz)	δ_{H} (600 MHz)	δ_{C} (150 MHz)
1		186.8 (s)		197.1 (s)
2		102.8 (s)		104.6 (s)
3		69.8 (s)		173.1 (s)
4		81.6 (s)		187.6 (s)
4-OH	9.63 (1H, s)			
5	8.69 (1H, d, 7.7)	127.9 (d)	8.24 (1H, dd, 7.7, 1.3)	130.8 (d)
6	7.62 (1H, t, 7.7)	134.1 (d)	7.67 (1H, td, 7.7, 1.3)	133.0 (d)
7	7.19 (1H, overlap)	128.6 (d)	7.63 (1H, td, 7.7, 1.3)	132.7 (d)
8	8.12 (1H, d, 7.7)	127.7 (d)	7.94 (1H, dd, 7.7, 1.3)	130.0 (d)
9		131.8 (s)		139.7 (s)
10		144.3 (s)		135.9 (s)
11	6.36 (1H, d, 5.7)	125.7 (d)	7.33 (1H, d, 5.8)	124.0 (d)
12	6.26 (1H, d, 5.7)	142.3 (d)	6.91 (1H, d, 5.8)	152.6 (d)
13		88.5 (s)		93.4 (s)
14	1.35 (3H, s)	28.9 (q)	1.53 (3H, s)	26.3 (q)
15	1.35 (3H, s)	27.5 (q)	1.31 (3H, s)	25.2 (q)
16		166.4 (s)		154.2 (s)
17	3.82 (3H, s)	52.3 (q)	3.88 (3H, s)	56.0 (q)
1'		187.6 (s) or 187.5 (s) ^c		138.4 (s)
2'		64.8 (s)		119.4 (s)
3'		68.8 (s)		118.7 (s)
4'		187.5 (s) or 187.6 (s) ^c		154.5 (s)
4'-OH			11.32 (1H, s)	
5'	7.77 (1H, overlap)	127.4 (d) or 127.1 (d) ^c	8.44 (1H, d, 8.3)	124.7 (d)
6'	7.43 (1H, overlap)	134.9 (d) or 134.8 (d) ^c	7.59 (1H, td, 8.3, 1.0)	126.8 (d)
7'	7.43 (1H, overlap)	134.8 (d) or 134.9 (d) ^c	7.69 (1H, td, 8.3, 1.0)	130.4 (d)
8'	7.77 (1H, overlap)	127.1 (d) or 127.4 (d) ^c	7.92 (1H, d, 8.3)	121.8 (d)
9'		133.0 (s) or 132.7 (s) ^c		130.1 (s)
10'		132.7 (s) or 133.0 (s) ^c		125.1 (s)

^aNMR data of **1** were recorded in C₅D₅N. ^bNMR data of **2** were recorded in CDCl₃. ^cMay be changeable for the signal overlapping.

and 64.8 (s). **1** was presumed to be a naphthoquinone dimer on the basis of these data.

Detailed interpretation of HMBC and ¹H–¹H COSY correlations (Figure S6, Supporting Information) allowed the construction of the fragments. The HMBC correlations from δ_{H} 8.12 (H-8) to δ_{C} 144.3 (C-10) and δ_{C} 186.8 (C-1); from δ_{H} 8.69 (H-5) to δ_{C} 131.8 (C-9) and δ_{C} 81.6 (C-4); from δ_{H} 9.63 (4-OH) to δ_{C} 81.6 (C-4) and δ_{C} 144.3 (C-10), together with the ¹H–¹H COSY correlations of H-5/H-6/H-7/H-8 gave a naphthohydroquinone moiety. Similarly, another naphthoquinone moiety was established based on the HMBC correlations from δ_{H} 7.77 (H-5' and H-8') to δ_{C} 133.0 and 132.7 (C-9' and C-10'), δ_{C} 187.6 and 187.5 (C-1' and C-4'), together with the ¹H–¹H COSY correlations of H-5'/H-6'/H-7'/H-8'. The HMBC correlations from δ_{H} 1.35 (H-14 and H-15) to δ_{C} 88.5 (C-13) and δ_{C} 142.3 (C-12); from δ_{H} 6.26 (H-12) to δ_{C} 69.8 (C-3); from δ_{H} 6.36 (H-11) to δ_{C} 102.8 (C-2), along with the ¹H–¹H COSY correlation of H-11/H-12, indicated an oxygen-contained spirocyclopentene group at C-3 position. The molecular formula and the remaining degrees of unsaturation suggested that **1** should possess heptacyclic system. Though the key HMBC correlation from δ_{H} 9.63 (4-OH) to δ_{C} 68.8 (C-3') gave a linkage of the two naphthoquinone moieties, the complete structure of **1** could not be established by NMR study because of the crowded quaternary carbons. Fortunately, a single crystal suitable for X-ray analysis was obtained after careful recrystallization in acetone. Thus, single-crystal X-ray diffraction was applied to

determine the final structure and absolute configurations of **1** (Figure 2). The results indicated that **1** occurs as a racemate,

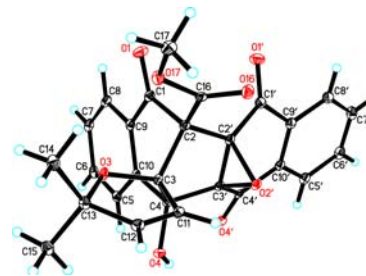


Figure 2. X-ray crystal structure of rubialatin A (**1**).

which was also confirmed by the $[\alpha]$ of zero. Subsequent analysis by a chiralpak IC column allowed separation of the enantiomers, (+)-**1** and (–)-**1** (Figure S17, Supporting Information). Since the absolute configurations of the enantiomers must be (2*R*, 3*R*, 4*S*, 2'*R*, 3'*S*)-**1** or (2*S*, 3*S*, 4*R*, 2'*S*, 3'*R*)-**1** according to the X-ray analysis, the absolute configuration of each enantiomer was then determined by calculation of the ECD spectrum using the time-dependent density functional theory (TD-DFT) method of the Gaussian 03 program package.¹⁸ The geometry was optimized at the B3LYP/CC-pVDZ level on the basis of the crystal structure by the density functional theory (DFT) method. The harmonic vibrational frequency was then calculated at the same level to

confirm its stability. The ECD spectrum for (2*R*,3*R*,4*S*,2'*R*,3'*S*)-**1** was further calculated at the B3LYP/CC-pVDZ level in methanol (Figure 3). The calculated ECD spectrum resembled

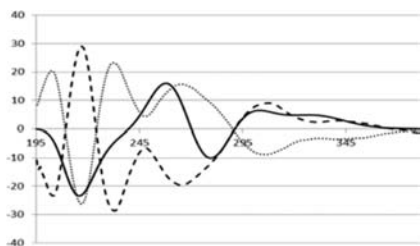


Figure 3. Calculated ECD spectrum of (2*R*,3*R*,4*S*,2'*R*,3'*S*)-**1** (solid); experimental ECD spectra of (+)-**1** (dash) and (–)-**1** (dot).

the experimental CD spectrum for (–)-**1**, which was opposite to that for (+)-**1**. Accordingly, the absolute configurations of the enantiomers were determined as (+)-(2*S*,3*S*,4*R*,2'*S*,3'*R*)-**1** and (–)-(2*R*,3*R*,4*S*,2'*R*,3'*S*)-**1**.

Compound **2** was obtained as yellow crystals (acetone). Its molecular formula was determined by HREIMS ($[M]^+$, 456.1194, calcd 456.1209) as $C_{27}H_{20}O_7$, which was in accordance with the 1H and ^{13}C NMR spectroscopic data (Table 1). The IR spectrum showed the absorptions at 3441, 3432, 1630, 1461 cm^{-1} , indicating the existence of hydroxyl, carbonyl, and phenyl groups. The 1H NMR spectrum showed two pairs of AA'BB' type aromatic protons at δ_H 8.24 (1H, dd, $J = 7.7, 1.3$ Hz), 7.94 (1H, dd, $J = 7.7, 1.3$ Hz), 7.67 (1H, td, $J = 7.7, 1.3$ Hz), 7.63 (1H, td, $J = 7.7, 1.3$ Hz), and 8.44 (1H, d, $J = 8.3$ Hz), 7.92 (1H, d, $J = 8.3$ Hz), 7.69 (1H, td, $J = 8.3, 1.0$ Hz), 7.59 (1H, td, $J = 8.3, 1.0$ Hz); two *cis* olefinic protons at δ_H 7.33 (1H, d, $J = 5.8$ Hz), 6.91 (1H, d, $J = 5.8$ Hz); one hydroxyl group at δ_H 11.32 (1H, s); one methoxyl group at δ_H 3.88 (3H, s); and two methyl groups at δ_H 1.53 (3H, s), 1.31 (3H, s). The ^{13}C NMR spectrum displayed two unsaturated ketonic carbonyl groups at δ_C 197.1 (s), 187.6 (s); one carbonyl group at δ_C 154.2 (s); 16 aromatic carbons at δ_C 154.5 (s), 139.7 (s), 138.4 (s), 135.9 (s), 133.0 (d), 132.7 (d), 130.8 (d), 130.4 (d), 130.1 (s), 130.0 (d), 126.8 (d), 125.1 (s), 124.7 (d), 121.8 (d), 119.4 (s), 118.7 (s); two olefinic carbons at δ_C 152.6 (d), 124.0 (d); one methoxyl group at δ_C 56.0 (q); two methyl groups at δ_C 26.3 (q), 25.2 (q); as well as three quaternary carbons at δ_C 173.1 (s), 104.6 (s), 93.4 (s). Compound **2** was also presumed to be a naphthoquinone dimer on the basis of these data.

Similar to **1**, 2D NMR also allowed the construction of the fragments rather than the complete structure (Figure S25, Supporting Information). The HMBC correlations from δ_H 7.94 (H-8) to δ_C 135.9 (C-10) and δ_C 197.1 (C-1); from δ_H 8.24 (H-5) to δ_C 139.7 (C-9) and δ_C 187.6 (C-4), together with the 1H – 1H COSY correlations of H-5/H-6/H-7/H-8 gave a 1,2-dicarbonyl substituted benzene moiety. The HMBC correlations from δ_H 1.53 (H-14) and δ_H 1.31 (H-15) to δ_C 93.4 (C-13) and δ_C 152.6 (C-12); from δ_H 7.33 (H-11) and δ_H 6.91 (H-12) to δ_C 93.4 (C-13) and δ_C 173.1 (C-3), along with the 1H – 1H COSY correlation of H-11/H-12, indicated the existence of an oxygen-contained cycloisopentene group. The HMBC correlations from δ_H 7.92 (H-8') to δ_C 125.1 (C-10') and δ_C 138.4 (C-1'); from δ_H 8.44 (H-5') to δ_C 154.5 (C-4'); from δ_H 11.32 (4'–OH) to δ_C 154.5 (C-4'), δ_C 118.7 (C-3') and δ_C 125.1 (C-10'), together with the 1H – 1H COSY correlations of H-5'/H-6'/H-7'/H-8' built a naphthoquinone moiety. Besides the correlations mentioned above, the

HMBC correlation from a methoxyl to a carbonyl group, δ_H 3.88 (H-17) to δ_C 154.2 (C-16), could be observed. The complete structure could not be elucidated by the NMR analysis for the lack of the linkage information on the fragments. Fortunately, single crystal was obtained after recrystallization in acetone. The single-crystal X-ray diffraction analysis showed the final structure (Figure 4).

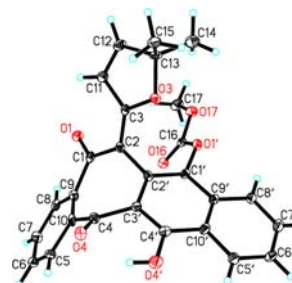


Figure 4. X-ray crystal structure of rubialatin B (**2**).

Compounds **1** and **2** showed unprecedented skeletons in natural products. Compound **1** has a novel 6/6/5/6/6 carbon skeleton coupled with a spirocycloisopentene group; **2** has a rearranged 6/7/6/6 tetracyclic system. They shared the same substructures, indicating that these compounds might originate from the same precursor, mollugin (**3**) (Figure S33, Supporting Information). The oxidation of **3** yielded (\pm)-**5**. Then the key intermediates (\pm)-**6** were derived from a series of nucleophilic coupling reactions between (\pm)-**5** and **4**. Compound **1** was produced by further oxidation of (\pm)-**6**, and **2** was formed from (\pm)-**6** by intramolecular rearrangements.

Compounds **1–3** were evaluated for their cytotoxicity against three human tumor cell lines (A549, SGC-7901, and HeLa) by the SRB method (Table 2).¹⁹ Compound **2** showed

Table 2. Cytotoxicity of Compounds **1–3** (IC₅₀, μM , Mean \pm SD)

	A549	SGC-7901	HeLa
(\pm)- 1	ND ^a	ND	ND
(+)- 1	ND	45.90 \pm 1.12	ND
(–)- 1	ND	ND	ND
2	25.63 \pm 0.74	10.74 \pm 0.65	13.08 \pm 0.38
3	ND	53.37 \pm 3.20	43.63 \pm 0.04
cisplatin	5.10 \pm 0.07	3.83 \pm 0.07	3.43 \pm 0.09

^aND: no detected ($>60 \mu M$).

cytotoxicity against these cell lines with the IC₅₀ values at 25.63, 10.74, and 13.08 μM . Interestingly, neither the racemic **1** nor (–)-**1** showed cytotoxicity, while (+)-**1** showed weak activity against SGC-7901 cell line with the IC₅₀ value at 45.90 μM . **3** showed weak cytotoxicity against SGC-7901 and HeLa cell lines too.

Compounds **1** and **2** were also evaluated for their effects on the NF- κB pathway (Figure 5).²⁰ Only compound (+)-**1** could inhibit TNF- α induced NF- κB activation at 40 μM (Figure 5A). But **2** could activate the NF- κB pathway with the existence of TNF- α , which revealed the synergistic effect of **2** with TNF- α on NF- κB activation (Figure 5B). Both NF- κB inhibition and activation have been reported to be relative to tumorigenesis.^{21,22} These results showed that (+)-**1** and **2** showed

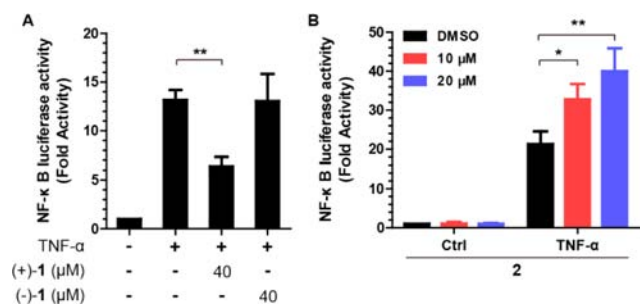


Figure 5. Effects of compounds **1** and **2** on TNF- α induced NF- κ B activation; * $p < 0.05$; ** $p < 0.01$.

cytotoxicity by different mechanisms, which need to be further investigated.

■ ASSOCIATED CONTENT

Supporting Information

Experimental procedures, bioactivity assays, 1D and 2D NMR, MS, UV, IR, $[\alpha]_D^{25}$, CD spectra, and X-ray crystal data (CIF) of rubialatins A (**1**) and B (**2**). This material is available free of charge via the Internet at <http://pubs.acs.org>.

■ AUTHOR INFORMATION

Corresponding Authors

*E-mail: nhtan@mail.kib.ac.cn.

*E-mail: gzh_zeng@mail.kib.ac.cn.

Author Contributions

§These authors contributed equally.

Notes

The authors declare no competing financial interest.

■ ACKNOWLEDGMENTS

This work was supported by the National Natural Science Foundation of China (U1032602, 30725048, 21102152), the National Basic Research Program of China (2013CB127505), the National New Drug Innovation Major Project of China (2011ZX09307-002-02), the Foundation of Chinese Academy of Sciences (Hundred Talents Program, XDA09030301-4), and the Natural Science Foundation of Yunnan Province (2012GA003, 2011FZ206). We are grateful to Prof. Bin Wu (Kunming Institute of Botany, CAS) for his valuable suggestions on the biogenetic pathway. We are also grateful to Prof. Heng Li (Kunming Institute of Botany, CAS) for identification of the plant. We also thank the members of the analytical group of the State Key Laboratory of Phytochemistry and Plant Resources in West China, Kunming Institute of Botany, for all of the spectral measurements.

■ REFERENCES

- (1) Tan, N. H.; Zhou, J. *Chem. Rev.* **2006**, *106*, 840–895.
- (2) Morita, H.; Takeya, K. *Heterocycles* **2010**, *80*, 739–764.
- (3) Zhao, S. M.; Kuang, B.; Fan, J. T.; Yan, H.; Xu, W. Y.; Tan, N. H. *Chimia* **2011**, *65*, 852–856.
- (4) Fan, J. T.; Chen, Y. S.; Xu, W. Y.; Du, L.; Zeng, G. Z.; Zhang, Y. M.; Su, J.; Li, Y.; Tan, N. H. *Tetrahedron Lett.* **2010**, *51*, 6810–6813.
- (5) Fan, J. T.; Su, J.; Peng, Y. M.; Li, Y.; Li, J.; Zhou, Y. B.; Zeng, G. Z.; Yan, H.; Tan, N. H. *Bioorg. Med. Chem.* **2010**, *18*, 8226–8234.
- (6) Huang, M. B.; Zhao, S. M.; Zeng, G. Z.; Kuang, B.; Chen, X. Q.; Tan, N. H. *Tetrahedron* **2014**, *70*, 7627–7631.

(7) Hitotsuyanagi, Y.; Kusano, J. I.; Kim, I. H.; Hasuda, T.; Fukaya, H.; Takeya, K. *Phytochemistry Lett.* **2012**, *5*, 335–339.

(8) Hitotsuyanagi, Y.; Odagiri, M.; Kato, S.; Kusano, J. I.; Hasuda, T.; Fukaya, H.; Takeya, K. *Chem.—Eur. J.* **2012**, *18*, 2839–2846.

(9) Singh, R.; Geetanjali; Chauhan, S. M. S. *Chem. Biodiversity* **2004**, *1*, 1241–1264.

(10) Itokawa, H.; Mihara, H.; Takeya, K. *Chem. Pharm. Bull.* **1983**, *31*, 2353–2358.

(11) Qiao, Y. F.; Takeya, K.; Itokawa, H.; Iitaka, Y. *Chem. Pharm. Bull.* **1990**, *38*, 2896–2898.

(12) Itokawa, H.; Ibraheem, Z. Z.; Qiao, Y. F.; Takeya, K. *Chem. Pharm. Bull.* **1993**, *41*, 1869–1872.

(13) Ibraheem, Z. Z.; Gouda, Y. G. *Bull. Pharm. Sci. Assiut Univ.* **2010**, *33*, 225–233.

(14) Fan, J. T.; Kuang, B.; Zeng, G. Z.; Zhao, S. M.; Ji, C. J.; Zhang, Y. M.; Tan, N. H. *J. Nat. Prod.* **2011**, *74*, 2069–2080.

(15) Kuang, B.; Han, J.; Zeng, G. Z.; Chen, X. Q.; He, W. J.; Tan, N. H. *Nat. Prod. Bioprospect.* **2012**, *2*, 166–169.

(16) Lumb, J. P.; Trauner, D. *J. Am. Chem. Soc.* **2005**, *127*, 2870–2871.

(17) Lumb, J. P.; Choong, K. C.; Trauner, D. *J. Am. Chem. Soc.* **2008**, *130*, 9230–9231.

(18) Frisch, M. J. Gaussian 03, Revision C.2; Gaussian, Inc., Wallingford, CT, 2004 (see the Supporting Information for the full reference).

(19) Zeng, G. Z.; Tan, N. H.; Ji, C. J.; Fan, J. T.; Huang, H. Q.; Han, H. J.; Zhou, G. B. *Phytother. Res.* **2009**, *23*, 885–891.

(20) Zhao, Y.; Su, J.; Goto, M.; Morris-Natschke, S. L.; Li, Y.; Zhao, Q. S.; Yao, Z. J.; Lee, K. H. *J. Med. Chem.* **2013**, *56*, 4749–4757.

(21) Sunwoo, J. B.; Chen, Z.; Dong, G.; Yeh, N.; Bancroft, C. C.; Sausville, E.; Adams, J.; Elliott, P.; Waes, C. V. *Clin. Cancer Res.* **2001**, *7*, 1419–1428.

(22) Kasperczyk, H.; Ferla-Brühl, K. L.; Westhoff, M. A.; Behrend, L.; Zwacka, R. M.; Debatin, K. M.; Fulda, S. *Oncogene* **2005**, *24*, 6945–6956.